Supporting Information for

Au-Decorated N-Rich Carbon Dots as Peroxidase Mimics for Detection of Acetylcholinesterase Activity

Dingding Zhang [a], Qingyi Han [a], Wendong Liu [a],Keying Xu [a], Mingzheng Shao [a], Yuyan Li [a], Peiyao Du [a], Zhen Zhang [a], Bingsi Liu [a], Libing Zhang [a]* and Xiaoquan Lu [b]**

[a] Tianjin Key Laboratory of Molecular Optoelectronic, Department of Chemistry, Tianjin University, Tianjin 300072, People's Republic of China

[b] Key Laboratory of Bioelectrochemistry and Environmental Analysis of Gansu Province, College of Chemistry and Chemical Engineering, Northwest Normal University, Lanzhou 730070, People's Republic of China

Materials, Instruments and Methods

Reagents and Materials.

$HAuCl_4$, polyethylene polyamine (PEPA), CH_3COOH, CH_3COONa, 1,2-diaminobenzene (OPD) , 2,2'-azino-bis(3-ethylbenzothiazoline-6-sulfonic acid) (ABTS) were all purchased from Shanghai Aladdin Biochemical Technology Co., Ltd. Acetylcholinesterase (AChE), Acetylthiocholine chloride (ATCh) were purchased from Shanghai Maclin Biochemical Technology Co., Ltd. Sodium hydrogen phosphate dihydrate, sodium dihydrogen phosphate anhydrous were purchased from Sun Chemical Technology (Shanghai) Co., Ltd. 3,3',5,5'-tetramethylbenzidine (TMB) was obtained from Shanghai Adamas Reagent Co., Ltd. Ultrapure water (≥18 MΩ, Millipore) was used in all experiments.

Instrumentation.

Transmission electron microscopy (TEM) measurements were made on a HITACHI H-8100 EM with an accelerating voltage of 200 kV. XPS measurement was performed on an ESCALAB-MKII spectrometer (VG Co., United Kingdom) with Al Kα X-ray radiation as the X-ray source for excitation. Fourier infrared spectra (FTIR) were recorded on Nicolet is5 (Thermo, USA). UV-Vis data were measured on UV-3600PLUS UV-Vis-NIR spectrophotometer (Shimazu Corporation, Japan). ICP-MS measurements were performed on Agilent 725 (USA), ESR were performed on Broker-A200 (Germany).

Synthesis of Cit-AuNPs (3 nm) and Cit-AuNPs (13 nm).

Cit-Au NPs (3 nm): [1]Au nanoparticles were obtained through adding 0.972 mL of 1% aqueous $HAuCl_4$ to 90 mL of H_2O in an ice bath under vigorous stirring, and then 2 mL of 1% aqueous

Na_3-citrate was added after 1 minute. After that, 1 mL of 0.075% $NaBH_4$ in 1% Na_3-citrate was also added. The solution was stirred for another 5 minutes and then stored at 4 °C. Thus the solution of 3 nm-diameter particles was synthesized successfully.

Cit-Au NPs (13 nm): [2]Briefly, a sodium citrate solution (0.1 M, 1.94 mL) was rapidly added to a boiled $HAuCl_4$ solution (50 mL H_2O, 0.0167g $HAuCl_4$) with vigorous stirring. The mixed solution was boiled for 10 min and further stirred for 15 min. The resulting wine-red solution was cooled to room temperature and filtered, which was stored in the 4 °C refrigerators before use.

Recyclability assessment.

50 mL Au-CDs (0.1 mg mL^{-1}), 50 mL H_2O_2 and 50 mL TMB were added to 350 mL HAc-NaAc and reacted at 30 ℃ for 15 min. Centrifuge the above-reacted solution at 14000 rpm for 15 min, discard the supernatant, and wash the bottom sediment with ultrapure water, redisperse the sediment in 50 mL of aqueous solution and perform the second test, and the subsequent steps are the same as above.

Steady-state kinetic assay of the Au-CDs.

Typically, 350 μL of acetate buffer (10 mM, pH 5.0), 50 μL of Au-CDs (0.1 mg mL^{-1}), 50 μL 200 mM H_2O_2, and 50 μL of TMB (0.1-4 mM) were mixed, followed by monitoring the reaction-time curves. Similarly, to obtain the kinetic data for H_2O_2, 350 μL of acetate buffer (10 mM, pH 5.0), 50 of μL Au-CDs (0.1 mg mL^{-1}), 50 μL of TMB (4 mM) and 50 μL H_2O_2 (1–1000 mM) were mixed.

Selectivity and anti-interference ability.

According to the acetylcholinesterase activity detection procedure, AChE was replaced with

different proteins to evaluate the selectivity of the sensing system, and other conditions remained the same. The activity of ALP and GOx is three times higher than AChE, the concentration of BSA is 0.1 mg mL^{-1}, and the concentration of other proteins is 0.2 mM. The anti-interference ability of the sensor system was evaluated by adding 50 μL different proteins into 30 μL ATCh.

Tables and Figures

Table S1. Au content in different solutions.

Sample	Au content (wt %)
Au-CD1	0.7
Au-CDs2	2.1
Au-CDs3	3.5
Au-CDs4	4.7
Au-CDs5	6.9
Au NPs (3 nm)	5.3
AuNPs (13 nm)	15.8

Table S2. Catalytic Parameters comparison of Au-CDs , HRP, and different Au-based catalyst.

Catalyst	Substrate	K_m (mM)	V_{max} ($10^{-8}M \cdot s^{-1}$)	Reference
HRP	H_2O_2	3.7	8.71	[3]
HRP	TMB	0.434	10	[3]
Tyr-Au NPs	H_2O_2	57.84	5.32	[4]
Tyr-Au NPs	TMB	0.024	0.91	[4]
citrate-Au NPs	H_2O_2	61.34	0.663	[5]
citrate-Au NPs	TMB	0.11	1.539	[5]
D-His@Au NCs	H_2O_2	72	5.55	[6]
D-His@Au NCs	TMB	0.41	7.69	[6]
BSA-Au NCs	H_2O_2	16.71	1.302	[7]
BSA-Au NCs	TMB	3.59	0.861	[7]
Au hydrogel	H_2O_2	19.92	12.8	[8]
Au hydrogel	TMB	0.32	12.30	[8]
ZnSA-AuAMP hydrogel	H_2O_2	30.53	1.679	[9]
ZnSA-AuAMP hydrogel	TMB	0.36	1.197	[9]
Au-CDs	H_2O_2	34.76	7.95	this work
Au-CDs	TMB	0.0196	1.282	this work

Table S3. Comparison of nanozyme-based biosensors for AChE detection.

Nanozymes	Method	Linear range (mU mL^{-1})	LOD (mU mL^{-1})	References
PAA-CeO_2	Fluorescence	0.263-50	0.263	[10]
Au@PDA NPs	Colormetric	2.5-25	0.9	[11]
RhB-p-SC_6A-AuNPs	Fluorescence	0-1.6	0.16	[12]
Citrate-CeO_2	Colormetric	0-1400	3.5	[13]
RhB-p-SC_6A-AuNPs	Colormetric	0-5	0.46	[12]
NO_2 -MIL-101	Colormetric	0.2-50	0.14	[14]
Fe-SAs/NC	Colormetric	2-70	0.56	[15]
PdSP@rGO	Colormetric	0.25-5.0	0.06	[16]
Au-CDs	Colormetric	0.1-5	0.107	This work
		0.6-10	0.157	
		1-17.5	0.192	

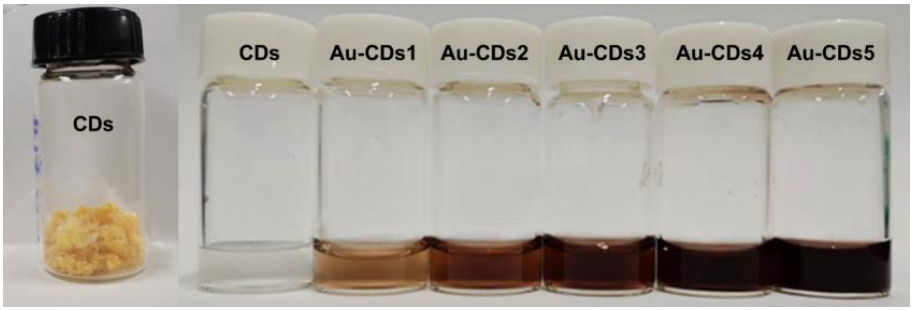

Figure S1. The digital photos of different products. The color of carbon dots and different Au-CDs solutions.

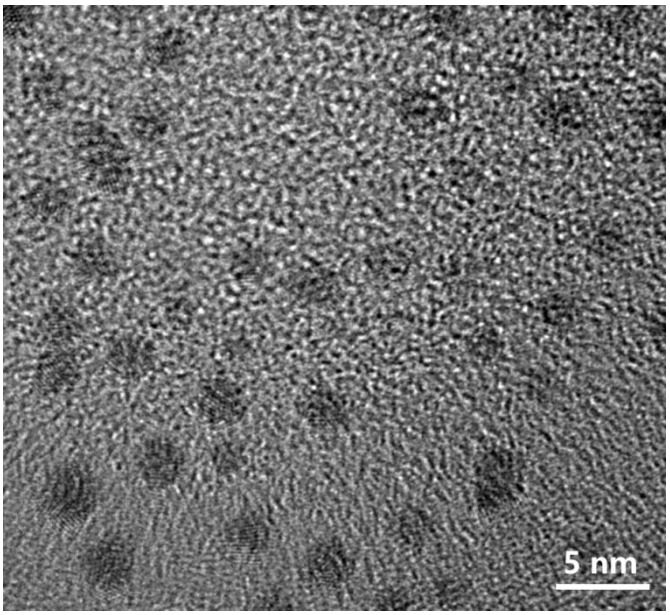

Figure S2. TEM image of Au-CDs stored at 4°C for one month.

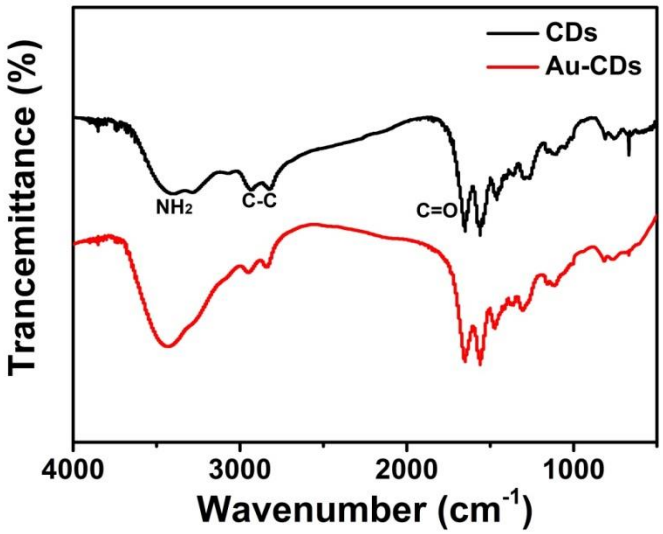

Figure S3. FTIR spectra of CDs and Au-CDs.

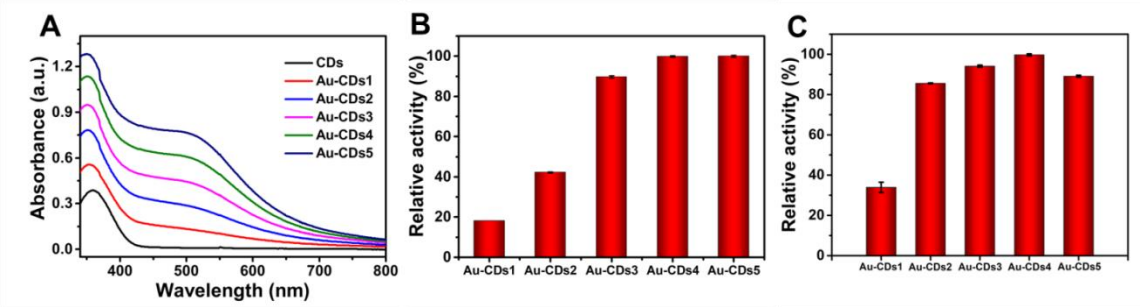

Figure S4. UV-vis spectra and relative activity of Au-CDs with different Au mass loadings. A) The UV-vis absorption of CDs and Au-CDs with different Au loadings; B) Relative activity of Au-CDs with different Au loadings for catalytic oxidation of TMB. C) Relative activity of different Au-CDs solutions with the same Au content for catalytic oxidation of TMB.

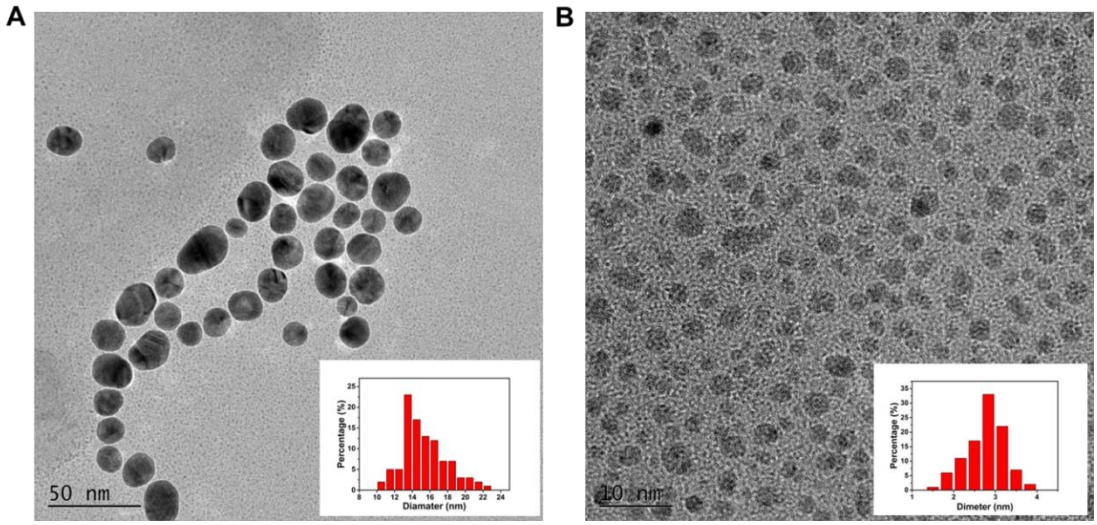

Figure S5. TEM images of Cit-Au NPs with different sizes. A) Cit-Au $NPs_{(13\ nm)}$ and B) Cit-Au $NPs_{(3\ nm)}$.

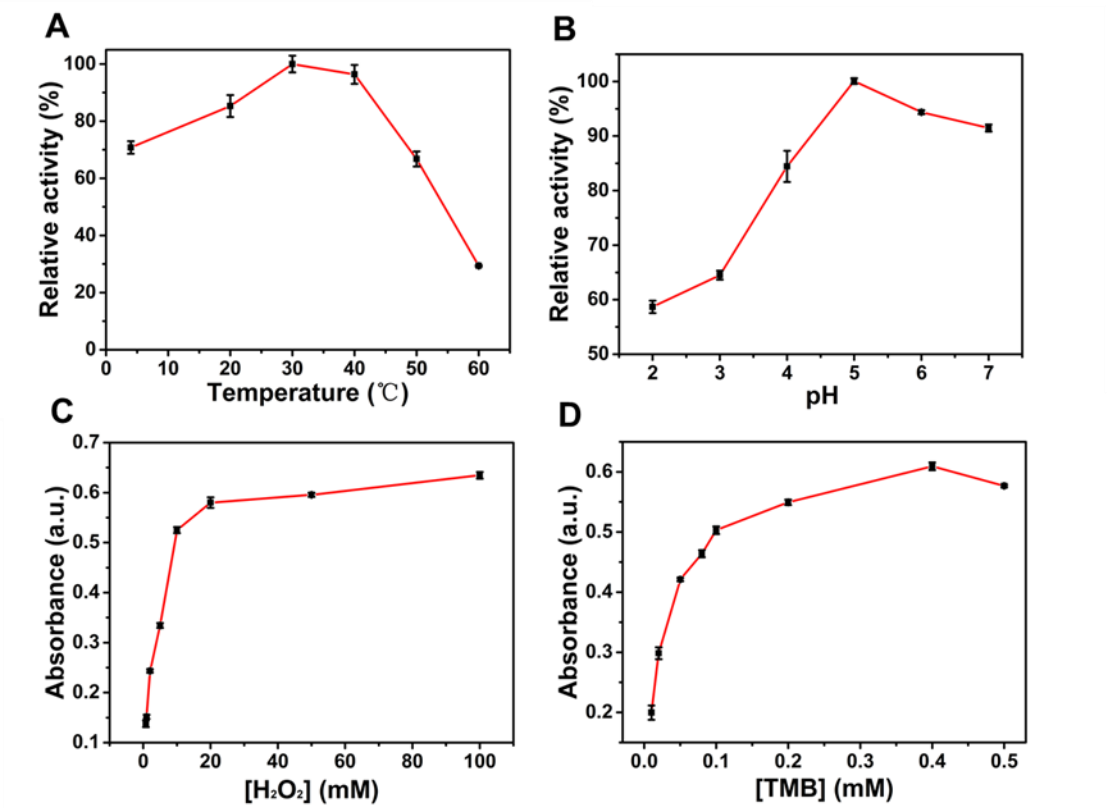

Figure S6. Optimization of Au-CDs reaction conditions. Peroxidase mimic activity of Au-CDs under different reaction conditions. A) reaction temperature; B) reaction system pH; C, D) concentration of H_2O_2 and TMB, respectively.

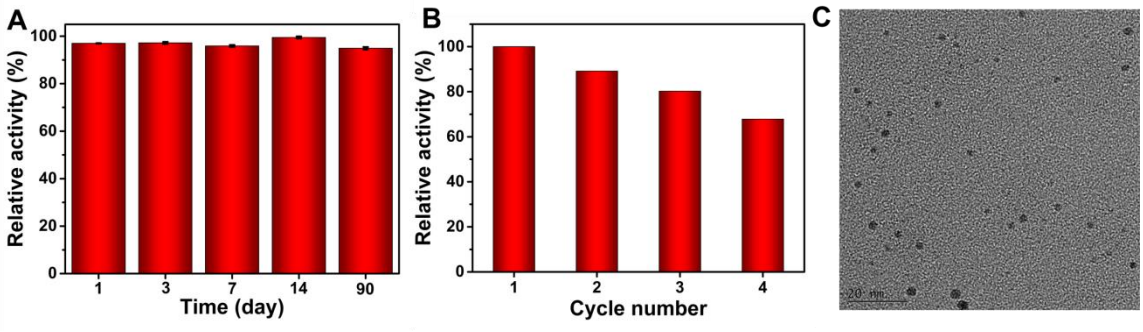

Figure S7. The stability and reusability of Au-CDs. A) The relative activity of Au-CDs at different storage times for catalytic oxidation of TMB. B) Cycle numbers of Au-CDs. C) TEM images of Au-CDs reacted with TMB and H_2O_2.

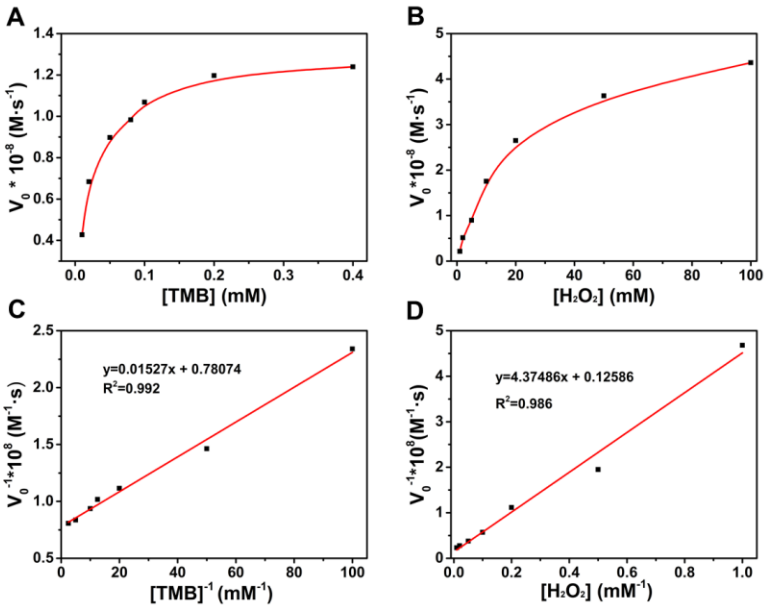

Figure S8. Kinetic analysis of Au-CDs with TMB and H_2O_2 as substrates. Michaelis-Menten curves fit of A) TMB with a fixed concentration of H_2O_2 (20 mM), B) H_2O_2 with a fixed concentration of TMB (0.4 mM). The Lineweaver-Burk plots for C) TMB and D) H_2O_2.

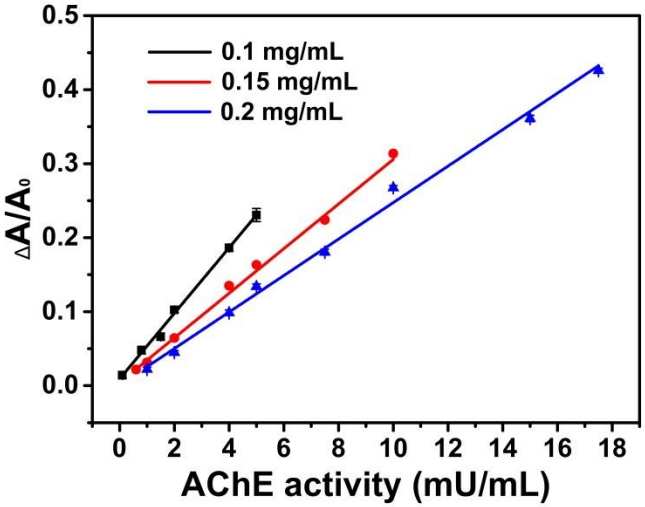

Figure S9. The linear response of Au-CDs to AChE at different concentration. The signal corresponds to the increase of AChE concentration. (The linear response of the sensing platform in the presence of increasing concentration of AChE, using three independent Au-CDs concentrations, respectively.)

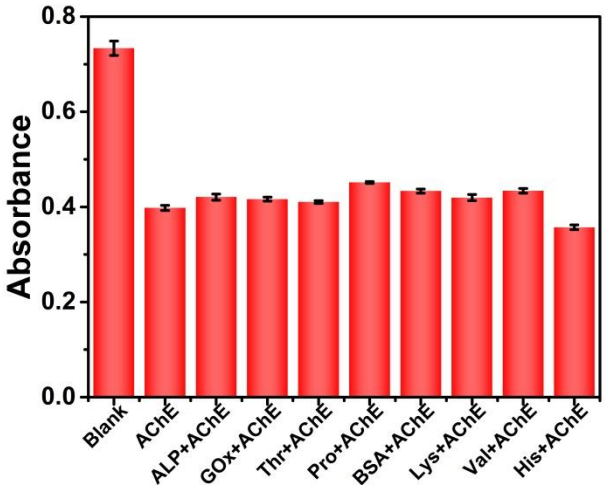

Figure S10. The anti-interference ability of Au-CDs for AChE detection.

References

[1] Xiao, X.-Y.; Chen, S.-H.; Li, S.-S.; Wang, J.; Zhou, W.-Y.; Huang, X.-J. Synergistic Catalysis of N Vacancies and ~5nm Au Nanoparticles Promoted the Highly Sensitive Electrochemical Determination of Lead(II) Using an Au/N-Deficient-C_3N_4 Nanocomposite. *Environ Sci-Nano.* **2019,** *6*, 1895-1908.

[2] Zhang, L.; Jean, S. R.; Li, X.; Sack, T.; Wang, Z.; Ahmed, S.; Chan, G.; Das, J.; Zaragoza, A.; Sargent, E.H.; Kelley, S.O. Programmable Metal/Semiconductor Nanostructures for mRNA-Modulated Molecular Delivery. *Nano Lett.* **2018,** *18*, 6222-6228.

[3] Gao, L.; Zhuang, J.; Nie, L.; Zhang, J.; Zhang, Y.; Gu, N.; Wang, T.; Feng, J.; Yang, D.; Perrett, S.; Yan, X. Intrinsic Peroxidase-Like Activity of Ferromagnetic Nanoparticles. *Nat. Nanotechnol.* **2007,** *2*, 577-583.

[4] Weerathunge, P.; Ramanathan, R.; Torok, V.A.; Hodgson, K.; Xu, Y.; Goodacre, R.; Behera, B. K.; Bansal, V. Ultrasensitive Colorimetric Detection of Murine Norovirus Using NanoZyme Aptasensor. *Anal Chem.* **2019,** *91*, 3270-3276.

[5] Xue, Q.; Niu, X.; Liu, P.; Wang, M.; Peng, Y.; Peng, H.; Li, X. Analyte-Triggered Citrate-Stabilized Au Nanoparticle Aggregation with Accelerated Peroxidase-Mimicking Activity for Catalysis-Based Colorimetric Sensing of Arsenite. *Sens Actuators B Chem.* **2021,** *334*, 129650.

[6] Song, Y.; Qiao, J.; Liu, W.; Qi, L. Colorimetric Detection of Serum Doxycycline with D-histidine-Functionalized Gold Nanoclusters as Nanozymes. *Analyst* **2020,** *145*, 3564-3568.

[7] Hu, L.; Liao, H.; Feng, L.; Wang, M.; Fu, W. Accelerating the Peroxidase-Like Activity of Gold Nanoclusters at Neutral pH for Colorimetric Detection of Heparin and Heparinase Activity. *Anal. Chem.* **2018,** *90*, 6247-6252.

[8] Jiao, L.; Xu, W.; Yan, H.; Wu, Y.; Gu, W.; Li, H.; Du, D.; Lin, Y.; Zhu, C. A Dopamine-Induced Au Hydrogel Nanozyme for Enhanced Biomimetic Catalysis. *Chem Commun (Camb).* **2019,** *55*, 9865-9868.

[9] Liu, L.; Jiang, H.; Wang, X. Alkaline Phosphatase-Responsive Zn^{2+} Double-Triggered Nucleotide Capped Gold Nanoclusters/ Alginate Hydrogel with Recyclable Nanozyme Capability. *Biosens. Bioelectron.* **2021,** *173*, 112786.

[10] Zhang, S. -X.; Xue, S. -F.; Deng, J.; Zhang, M.; Shi, G.; Zhou, T. Polyacrylic Acid-Coated Cerium Oxide Nanoparticles: An Oxidase Mimic Applied for Colorimetric Assay to Organophosphorus Pesticides. *Biosens. Bioelectron.* **2016,** *85*, 457-463.

[11] Zhang, J.; Mou, L.; Jiang, X. Hydrogels Incorporating Au@Polydopamine Nanoparticles: Robust Performance for Optical Sensing. *Anal. Chem.* **2018, 90**, 11423-11430.

[12] Lv, J.; He, B.; Wang, N.; Li, M.; Lin, Y. A Gold Nanoparticle Based Colorimetric and Fluorescent Dual-Channel Probe for Acetylcholinesterase Detection and Inhibitor Screening. *RSC Adv.* **2018,** *8*, 32893-32898.

[13] Cheng, H.; Lin, S.; Muhammad, F.; Lin, Y.-W.; Wei, H. Rationally Modulate the Oxidase-like Activity of Nanoceria for Self-Regulated Bioassays. *ACS Sens.* **2016,** *1*, 1336-1343.

[14] Xu, W.; Kang, Y.; Jiao, L.; Wu, Y.; Yan, H.; Li, J.; Gu, W.; Song, W.; Zhu, C. Tuning Atomically Dispersed Fe Sites in Metal-Organic Frameworks Boosts Peroxidase-Like Activity for Sensitive Biosensing. *Nano-Micro Lett.* **2020,** *12*, 184.

[15] Wang, M.; Liu, L.; Xie, X.; Zhou, X.; Lin, Z.; Su, X. Single-Atom Iron Containing Nanozyme with Peroxidase-Like Activity and Copper Nanoclusters Based Ratio Fluorescent Strategy for Acetylcholinesterase Activity Sensing. *Sens Actuators B Chem.* 2020, *313*, 128023.

[16] Yan, B.; Liu, W.; Duan, G.; Ni, P.; Jiang, Y.; Zhang, C.; Wang, B.; Lu, Y.; Chen, C. Colorimetric Detection of Acetylcholinesterase and its Inhibitor based on

Thiol-Regulated Oxidase-Like Activity of 2D Palladium Square Nanoplates on Reduced Graphene Oxide. *Microchim Acta.* **2021,** *188,* 162.